J. Chem. Thermodynamics **1980,** 12, 717–736

Thermodynamics of some lanthanide trihalides III. Reinterpretation of $LnCl_3$ Schottky anomalies [a]

EDGAR F. WESTRUM, JR., ROBERT D. CHIRICO,[b]

Department of Chemistry, University of Michigan, Ann Arbor, Michigan 48109, U.S.A.

and

JOHN B. GRUBER

Department of Physics, North Dakota State University, Fargo, North Dakota 58102, U.S.A.

(*Received 6 August 1979*)

The heat capacities of the anhydrous lanthanide trichlorides from 5 to 350 K of Sommers and Westrum provide an excellent opportunity further to test the volumetric lattice heat-capacity approximation method. Schottky contributions in $PrCl_3$, $SmCl_3$, and $EuCl_3$ were calorimetrically derived using the volume-weighted interpolation between the lattice heat capacities of the La and Gd homologs. Previously qualitative agreement had been observed upon comparison of these calorimetrically derived Schottky contributions with those calculated from spectroscopic data obtained for Ln(III)-doped $LaCl_3$ crystals. Excellent accord between "spectroscopic" and "calorimetric" Schottky contributions is achieved by adjusting the Stark-level energies to represent those of the concentrated salts through extrapolation of the Ln(III)-doped $LaCl_3$ energies to stronger crystal fields either empirically or by means of estimated crystal-field parameters. These methods are described and the resulting energy levels are compared with the extant spectroscopic results for the concentrated trichlorides. In addition, new electronic-Raman-scattering determinations were made on $PrCl_3$ and $SmCl_3$ at 15 K and vibrational Raman lines are reported for $SmCl_3$ at 300 K. Deduced electronic energy levels for the ground and first excited [SL]J-manifolds are listed for both compounds.

1. Introduction

Excellent resolution of the Schottky contributions to the heat capacities of $Pr(OH)_3$,[1] $Eu(OH)_3$,[2] and $Tb(OH)_3$,[3] have recently been achieved by means of a vibrational ("lattice") heat-capacity approximation based upon an interpolation between the lattice heat capacities of the lanthanum and gadolinium homologs weighted by the fractional molar-volume variation along the series. The heat

[a] This research was supported in part by the Structural Chemistry and Chemical Thermodynamics Program of the Chemistry Section of the National Science Foundation under contract GP-42525X. Papers I and II in this Series are references 4 and 5.

[b] Present address: Department of Chemistry, University of Illinois at Chicago Circle, Chicago, Illinois, U.S.A.

0021-9614/80/080717+20 $01.00/0

capacities of the anhydrous lanthanide trichlorides from 5 to 350 K of Somers and Westrum[4,5] (papers I and II of this series) plus the wealth of spectroscopic data which were the primary impetus for the original investigation,[6] provide an excellent opportunity further to test the new lattice heat-capacity estimation scheme.

Traditionally the success of a lattice heat-capacity approximation has been judged in terms of the agreement between the Schottky contribution calculated from electronic spectral data (the "spectroscopic" Schottky contribution) and that deduced calorimetrically using the lattice heat-capacity approximation in question (the "calorimetric" Schottky contribution). Application of this criterion is complicated by the fact that the spectroscopically determined energy levels are often obtained for the paramagnetic ion of interest doped into a diamagnetic host lattice (commonly the La or Y analog) rather than for the concentrated salt. Increments of 20 cm^{-1} for individual Stark wavenumbers are not uncommon between doped and concentrated salts. Moreover, since variation of the Stark-level energies with temperature is not taken into account, perfect agreement between the "spectroscopic" and "calorimetric" Schottky contributions is an unrealizable expectation—discounting coincidence—even if the lattice contributions were precisely known. Indeed, we here show that the energy levels of Ln^{3+}-doped $LaCl_3$ are inadequate for precise calculations of the Schottky heat capacity of the light anhydrous lanthanide trichlorides.

The primary cause of the observed energy-level shifts between the doped and concentrated crystals may be rationalized as follows. The lanthanide contraction insures that the lanthanum analog has the largest cation-to-anion separations in any lanthanide series. This implies that the smaller paramagnetic ions doped into the lattice of the lanthanum analog will be subject to a relatively weak crystalline field in comparison to that within the concentrated paramagnetic compound. Some local distortion at the dopant site in the diamagnetic host lattice is anticipated; however, Cohen and Moos[7,8] have observed the vibronic spectra of Pr^{3+} ions in a series of lanthanide-trichloride host lattices and have found the Pr^{3+} dopant ions to be subject to the same environment as the host-lattice cations and to produce little local distortion. The weaker crystalline field of the lanthanum-analog host lattice is expected to decrease the observed splitting of the individual J-manifolds and simultaneously to increase slightly the separation between their centers of gravity. Although rare exceptions may be found,[9] the available experimental evidence is in accord with these expectations. In this paper it will be shown that the effect of these energy-level shifts may be clearly observed in the heat capacities of the concentrated trichlorides upon application of the new lattice-approximation technique. Due to an overshadowing uncertainty in the lattice heat-capacity contribution, this effect had been undetected until now.

Two techniques are described for adjustment of the Stark-level energies of Ln^{3+}-doped $LaCl_3$ so as to approximate those of the concentrated paramagnetic salts. These techniques are based upon the observed discrepancy between the spectroscopic Schottky contribution calculated from Ln^{3+}-doped $LaCl_3$ energy levels and the calorimetric Schottky curve derived using the new lattice approximation. The adjustments are performed, first, by a near-linear extrapolation of the Ln^{3+}-doped

$LaCl_3$ energies to stronger crystal fields and, secondly, by means of estimated crystal-field parameters. These methods are described in detail and the derived energy levels are compared with previously unpublished electronic Raman scattering spectra for concentrated $SmCl_3$ and $PrCl_3$, and absorption spectra for concentrated $NdCl_3$.

Electronic Raman (two-photon) scattering has been observed in few instances in lanthanide crystals. The observed Raman effect usually has been associated with the lattice vibrations of the crystal.[10-12] An early report on the electronic Raman lines observed in hydrated samarium nitrate was later shown to be in error.[13,14] More recently, Hougen and Singh[15] observed the electronic Raman effect for concentrated $PrCl_3$. Elliott and Loudon[16] also suggested the possibility of observing the Stark splitting of the ground and low-lying excited [SL]J-manifolds of lanthanide ions in crystals. Shortly thereafter Axe,[17] using tensor operators originally developed by Judd,[18] was able to show that the observed electronic Raman intensities reported by Hougen and Singh[15] could be understood quantitatively in terms of reduced matrix elements.

Crystal spectra of tripositive lanthanides ($4f^n$) and tripositive actinides ($5f^n$) have been studied in some depth for many years using various absorption and fluorescence techniques.[6,19-21] With the advent of the laser, a new excitation source became available bringing with it high intensity and power density, as well as monochromaticity and coherence.[22,23] These source characteristics revived interest in multiphoton processes and set the stage for new and exciting inquiries into two-photon absorption as well as Rayleigh and Raman scattering experiments.[24-27] The theoretical foundation for such studies was given by Dirac.[28] Two-photon absorption and emission were treated by Goeppert-Mayer[29] who made use of time-dependent perturbation theory in quantum mechanics. Two-photon spectroscopy is particularly suited to studying $n'f^n \rightarrow n'f^n$ electronic transitions since two-photon interaction matrix-elements in the electric-dipole approximation achieve their maximum probability between states of the same parity. Two-photon excitation processes in rare earths have been reported by Kaiser and Garrett,[30] by Richman and Chang,[31] by Schaak and Konigstein,[32] and by Bayer and Schaack.[33] Theoretical predictions and calculations for two-photon excitation in lanthanides have been reported by Kleinman,[34] by Axe,[17] as well as by Stoner and Gruber;[35] general remarks and reviews of the theoretical implications have been given by a variety of authors.[36-40]

Selection rules for two-photon absorption and electronic Raman scattering are in many cases different from those associated with single-photon processes so that Stark levels have been detected and identified that otherwise would not have been observed using the traditional absorption and fluorescence techniques. Moreover, detection of the CEF splitting of lanthanide-ion electronic levels in concentrated salts—including insulators and some metallic vapors—is possible using Raman scattering techniques without the complexities of broadened bands and satellite structure.

The present re-evaluation and re-interpretation of the Schottky contributions to the heat capacities of the light anhydrous lanthanide trichlorides further reveals the validity of the new lattice-approximation method. The accompanying spectra for the concentrated salts substantiate the re-interpretation.

2. The Schottky heat-capacity function

The average energy $\langle E \rangle$ of a system with energy levels ε_i and corresponding degeneracies g_i can be written:

$$\langle E \rangle = \left\{\sum_i \varepsilon_i g_i \exp(-\varepsilon_i/kT)\right\} / \left\{\sum_i g_i \exp(-\varepsilon_i/kT)\right\},$$

in which k and T are the Boltzmann constant and the temperature. The molar heat capacity is given by

$$C_x/R = \left\{\sum_i g_i(\varepsilon_i/kT)^2 \exp(-\varepsilon_i/kT)\right\}/Z - \left[\left\{\sum_i g_i(\varepsilon_i/kT)\exp(-\varepsilon_i/kT)\right\}/Z\right]^2. \quad (1)$$

The x in the above expression represents any parameter upon which the energy levels and their degeneracies depend; Z is the electronic partition function. If the electronic energy levels and degeneracies of the system are known, equation (1) can be used to calculate the Schottky heat-capacity contribution. For lanthanide compounds these are most commonly available from optical spectroscopy.

The properties of the Schottky heat-capacity function for a simple system involving only two energy levels separated by an energy ε are well known.[41] If sets of energy levels arising from a single multidegenerate state are proportional to some parameter $\omega > 0$, the maxima of the derived Schottky heat capacities of the sets are independent of ω. Moreover, the fractional shift in the temperature of the Schottky maximum is identical to the fractional shift in ω and, hence, identical to the fractional shifts in the energies of the contributing levels. The energy levels which are principally responsible for the Schottky heat capacity below 350 K for nearly all lanthanide compounds, indeed, do arise from a single multidegenerate state; the lowest lying [SL]J-state. The Eu(III) analog is the exception to this generalization within a series of analogous compounds.

Although the effect of the crystal field in the light lanthanide trichlorides is defined by four "crystal-field" parameters,[6] the one-parameter approximation can be a useful tool if its limitations are appreciated. For example, the calculated Schottky heat capacities of $Er(OH)_3$, Er^{3+}-doped $GdCl_3$, and Er^{3+}-doped $LaBr_3$ (chosen because all of the crystals consist of hexagonal unit cells containing two molecules within which the Er^{3+} ions are located at sites of C_{3h} point symmetry) have nearly identical maxima (*i.e.* within $0.015C_p/R$). This suggests that the crystal-field splitting of the ground($^4I_{15/2}$) J-manifold of these Er(III) compounds may indeed be expressed in terms of a single parameter. Figure 1(a) clearly shows this to be true. The position of the sets of Stark levels along the abscissa of figure 1(a) is quantitatively defined by the relative temperatures of the Schottky maxima. No exact functional relationship exists between the parameter ω and the crystal-field intensity; however, this does not affect the interpretation. The compounds used in the above example represent a wide range of crystal-field intensities; yet a counter example is provided by $Er(EtSO_4)_3 \cdot 9H_2O$, which would appear to be an ideal addition to this group; however, due to the bulky ethyl-sulfate ligands attached to the Er^{3+} ions, steric effects play an important role in determining the crystal-field intensity experienced by the

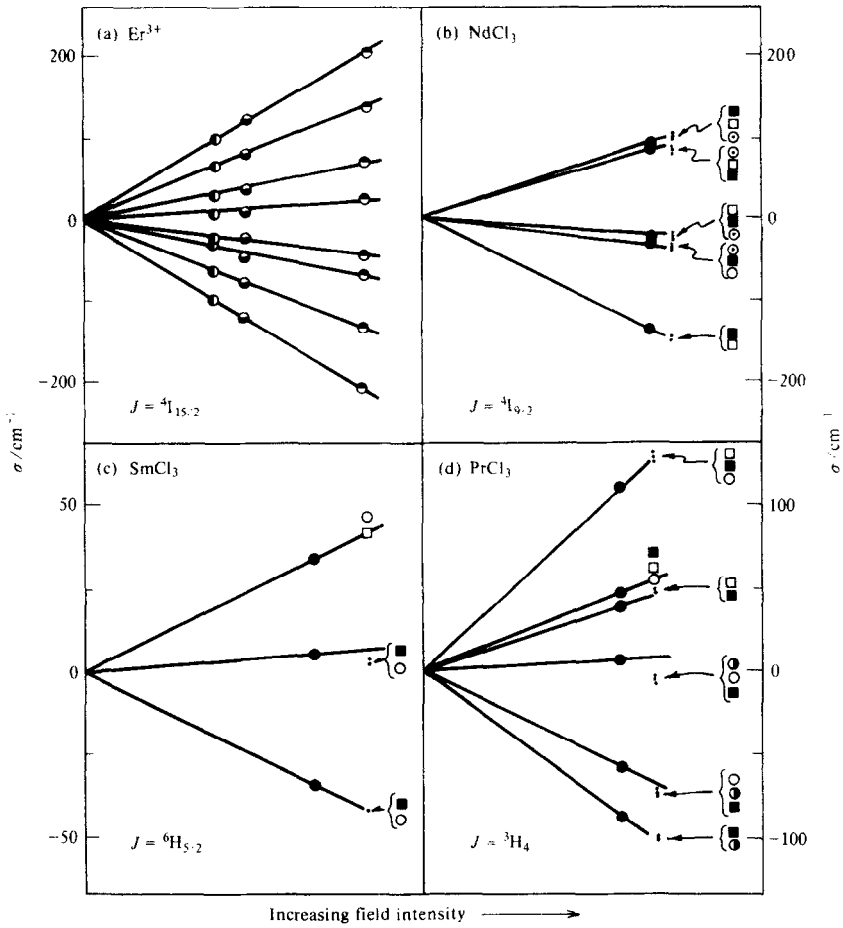

FIGURE 1. Crystal-field splitting of the ground-state J-manifolds of concentrated and lanthanide-ion doped lanthanide(III) compounds. ◐, ◒, ◓, the spectroscopically determined wavenumbers of the Er^{3+} ion in $LaBr_3$, $GdCl_3$, and $Er(OH)_3$, respectively. ●, Ln^{3+}-doped $LaCl_3$ wavenumbers; □, calorimetrically deduced wavenumbers of the concentrated $LnCl_3$'s (see text); ■, wavenumbers calculated from estimated crystal-field parameters for the concentrated $LnCl_3$'s (see text); ○, wavenumbers derived from the electronic Raman scattering experiments of this research. ⊙, ◑, the wavenumbers of concentrated $NdCl_3$ and $PrCl_3$, deduced from absorption spectra by Prinz[48] and by Dorman,[51] respectively.

erbium ions. The maximum of the Schottky heat capacity of $Er(EtSO_4)_3 \cdot 9H_2O$ is, in fact, about $0.20C_p/R$ lower than those of the first three compounds.

The properties of the Schottky heat capacities of complex systems, described above, are exploited in estimating the crystal-field splitting of the concentrated light lanthanide trichlorides from calorimetric Schottky contributions derived using the new lattice-contribution estimate and the crystal-field splitting observed for the corresponding Ln^{3+}-doped $LaCl_3$ crystals.

3. The lattice heat capacity

Within any trivalent lanthanide series, not only the (total) observed heat capacities of the diamagnetic La(III) and Lu(III) end-members but also that of the Gd(III) analog may be considered to entail only a lattice contribution above about 25 K. Below this temperature the cooperative magnetic contribution associated with the ordering of the Gd^{3+} ions becomes increasingly large and ultimately culminates in a λ-type transition—generally below 5 K—with a total associated entropy of (R ln 8). Above the critical temperature the cooperative magnetic contribution may be expressed as the power series:[42]

$$C(\text{magnetic})/R = \sum_{n=2}^{\infty} C_n/T^n.$$

If the coefficients C_n are known, the cooperative magnetic contribution may be calculated and deducted from the total heat capacity of the Gd(III) analog, thus extending the knowledge of the lattice contribution to lower temperatures. Clover and Wolf[43] have shown that the C_2 and C_3 terms are sufficient for calculation of the cooperative magnetic contribution to the total heat capacity of $GdCl_3$ above 5 K. The C_2 and C_3 values deduced by Clover and Wolf are $(3.36 \pm 0.01)\ K^2$ and $-(5.3 \pm 0.4)\ K^3$, respectively.

The difference between the total heat capacities of $LaCl_3$ and $GdCl_3$ (depicted in figure 2) may be considered to represent the total variation of the lattice heat capacity across the light lanthanide-trichloride series. Clearly, resolution of the excess

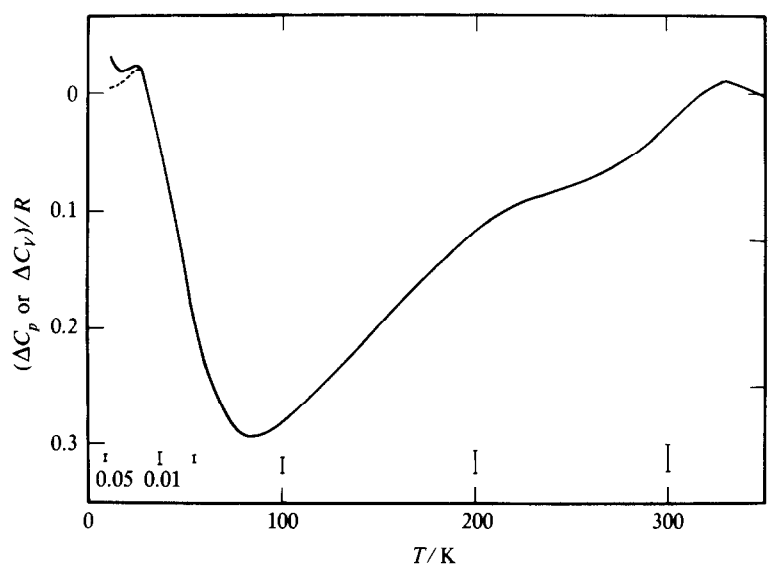

FIGURE 2. The solid curve represents the difference $\Delta C_p = \{C_p(GdCl_3) - C_p(LaCl_3)\}$. The dashed curve represents the same difference after deletion of the cooperative magnetic contribution to the heat capacity of $GdCl_3$. Error bars (unless noted otherwise) represent $0.002C_p(LaCl_3)$.

electronic (Schottky) heat capacity of the intermediate series members requires a basis for interpolation of the lattice heat capacity along the series between the $LaCl_3$ and $GdCl_3$ homologs. Excellent resolution of the Schottky contributions for several lanthanide trihydroxides is achieved[1-3] when the interpolation between the La(III) and Gd(III) analogs is weighted by the fractional molar-volume variation along the series. The corresponding formulae for the lattice heat capacities of the light anhydrous lanthanide trichlorides are

$$C_p(\text{lattice, } LnCl_3) = (1-f)\{C_p(LaCl_3)\} + f\{C_p(GdCl_3)^*\},$$

in which f may be expressed in terms of the molar volumes V_i of the homologous light lanthanide trichlorides as

$$f = f(LnCl_3) = \{V(LnCl_3) - V(LaCl_3)\}/\{V(GdCl_3) - V(LaCl_3)\}. \quad (2)$$

The values of $f(LnCl_3)$ are based upon the mean of the lattice parameters available in the literature.[4, 5] The asterisk indicates that the heat capacity associated with the cooperative antiferromagnetic ordering of $GdCl_3$ has been deleted. (A crystal structure change after $GdCl_3$ precludes direct application of this lattice-approximation technique to the heavier series members.) In the following section this lattice-approximation method is employed in the derivation of the calorimetric Schottky contributions to the heat capacities of $EuCl_3$, $NdCl_3$, $SmCl_3$, and $PrCl_3$.

4. The Schottky contributions to the $LnCl_3$ heat capacities

$EuCl_3$. The Schottky contribution to the heat capacity of the Eu(III) analog within the trivalent lanthanide series is unique in that it arises entirely from thermal population of excited [SL]J-manifolds. The wave number of the first excited [SL]J-state ($^7F_1$) of the Eu^{3+} ion is near 370 cm^{-1}. This invariably results in the lowest excited Stark levels for the Eu(III) analog being much higher in energy than for other series members. Therefore, as discussed,[2] the Schottky heat capacities of Eu(III) compounds are relatively insensitive to small errors or shifts in the Stark level energies. Consequently, good to excellent agreement between the spectroscopic and calorimetric Schottky contributions should be observed provided that an adequate estimation of the lattice contribution is available.

The energy levels of (1 and 4 mass per cent) Eu^{3+}-doped $LaCl_3$ were determined from the absorption spectrum at 4 K and the fluorescent spectrum at 4 and 77 K by Deshazer and Dieke.[44] The Stark-level energies arising from the first three [SL]J-states are listed in table 1. The $^7F_3$ Stark levels were also included in the spectroscopic Schottky calculation, although they are not listed. The Eu^{3+}-doped $LaCl_3$ spectroscopic Schottky contribution is shown as a solid line in figure 3.

The energy levels of Eu^{3+}-doped $LaCl_3$ are not expected to be identical to those of concentrated $EuCl_3$ due to the weaker crystal field within the $LaCl_3$ host. The largest contribution to the Schottky heat capacity below 350 K arises from population of the two $^7F_1$ Stark components. The stronger crystal field of concentrated $EuCl_3$ is expected to increase the Stark splitting and simultaneously to lower the center of gravity of the $^7F_1$ [SL]J-manifold. The anticipated net effect is to lower the energy of

TABLE 1. Wavenumbers σ of lanthanide trichlorides

$LnCl_3$	[SL]J-state		σ/cm^{-1}					
			Ln^{3+}-doped $LaCl_3$		Concentrated $LnCl_3$			
		μ[a]	Abs. fluor.[b]	Calorim.[c]	CEF[d]	ERS(I)[e]	ERS(II)[f]	Absorp.[g]
$EuCl_3$	$^7F_0$	0	0[h]					
	$7F_1$	1	355.05					
		0	405.27					
	$^7F_2$	2	1022.54					
		1	1027.54					
		0	1084.33					
$NdCl_3$	$^4I_{9/2}$	5/2	0[i]	0	0			0[j]
		1/2	115.39	122	123			123.74
		3/2	123.21	135	131			129.6
		5/2	244.4	255	246			260
		3/2	249.4	265	268			261
$SmCl_3$	$^6H_{5/2}$	1/2	0[k]	0	0	0		
		3/2	40.7	50	50	47		
		5/2	66.1	88	88	(79) (93)	wk.	
	$^6H_{7/2}$	3/2	992.8			987		
		5/2	1051.2			1047		
		1/2	1104.7			1108		
		5/2	1172.6			1180		
$PrCl_3$	$^3H_4$	2	0[l]		0	0	0	0[m]
		3⁻	33.1		29	30.5	32	31.8
		2′	96.4		99	99	100	99.6
		1	130.2	155	152	145	139	
		3⁺	137.0	168	176	160		
		0	199.1	235	230	(228)		
	$^3H_5$	3⁻	2137.2			2134	2136	
		2	2169.8			2168	2169	2167
		1	2188.5			2190	2190	2191
		3⁺	2202.2			2208	2204	
		2	2222.6			2230	2227	2230
		1				2260		
		0						

[a] Assigned crystalline-field quantum numbers. [b] Absorption and/or fluorescence spectra. [c] Deduced calorimetrically through application of the lattice heat capacity interpolation method (see text). [d] Calculated from estimated crystal-field parameters (see text). [e] Electronic Raman scattering values of this research. [f] Electronic Raman scattering values of Hougen and Singh.[15] [g] Absorption spectra. [h] DeShazer and Dieke.[44] [i] Carlson and Dieke.[45,46] [j] Prinz.[47,48] [k] Magno and Dieke.[49] [l] Sarup and Crozier.[50] [m] Dorman.[51]

the $\mu = 1$ doublet and to leave the $\mu = 0$ level essentially unchanged. The effect of the stronger crystal field will be countered to some extent by expansion of the $EuCl_3$ lattice at higher temperatures (*i.e.* in the region of the Schottky maximum); however, this is anticipated to be insufficient fully to nullify the effect. Because the energies of the Stark levels contributing to the Schottky heat capacity are relatively high, a shift of the $\mu = 1$ ($^7F_1$) doublet by as much as 10 to 15 cm^{-1} will have only a very small effect on the calculated Schottky contribution. Hence, the Schottky contribution calculated from the energy levels of Eu^{3+}-doped $LaCl_3$ should provide an excellent approximation to the Schottky contribution for concentrated $EuCl_3$.

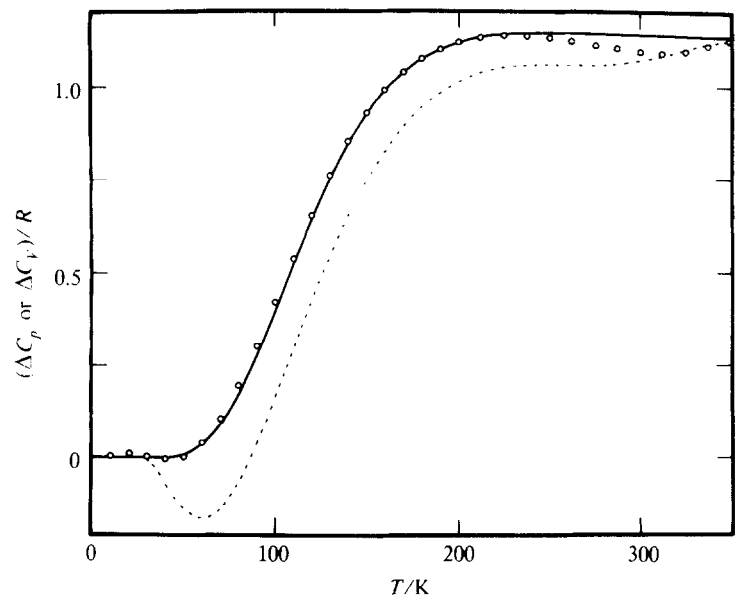

FIGURE 3. The Schottky contribution for $EuCl_3$. ———, Eu^{3+}-doped $LaCl_3$ spectroscopic Schottky contribution; ○, $EuCl_3$ calorimetric Schottky contribution; · · ·, $\Delta C_p = \{C_p(EuCl_3) - C_p(LaCl_3)\}$.

The lattice heat capacity of $EuCl_3$ was approximated by the weighted sum:

$$C_p(\text{lattice}, EuCl_3) = 0.12C_p(LaCl_3) + 0.88C_p(\text{lattice}, GdCl_3).$$

The weighting factors were determined using equation (2). The derived calorimetric Schottky heat capacity is shown in figure 3 (represented by the open circles) as is the difference (represented by the dotted curve) obtained when the heat capacity of $LaCl_3$ is subtracted from that of $EuCl_3$. The difference between these curves is due to the variation of the lattice heat capacities across the series. The agreement between the calorimetric and spectroscopic $EuCl_3$ Schottky contributions is seen to be excellent below approximately 230 K. Between 230 and 350 K the calorimetric Schottky contribution passes through a minimum that is not reproduced by the calculated curve. The anticipated shift of the $\mu = 1$ ($^7F_1$) level to lower energies would cause the calorimetric Schottky curve to be low in this temperature region; however, the observed effect is much too large for this to be the sole cause. (Nearly identical downward trends near 230 K were also observed in the $NdCl_3$ and $SmCl_3$ calorimetric Schottky heat capacities, as shown in figures 4 and 5; a much smaller effect was observed for $PrCl_3$.) A breakdown of the lattice-approximation method cannot be discounted; however, the observed deviation may be due to errors in the heat capacities determined in this temperature region as seen in figure 2. Moreover, it is extremely unlikely that the lattice heat capacity would undergo a change as sudden as that implied by the calorimetric Schottky curve between 250 and 350 K.

$NdCl_3$. The Schottky contribution to the heat capacity of neodymium(III) compounds below 350 K is due almost entirely to thermal population of excited

Stark levels within the $^4I_{9/2}$ ground [SL]J-manifold. The center of gravity of the first excited [SL]J-manifold ($^4I_{11/2}$) is at approximately 2100 cm^{-1}. Consequently, these levels make only a small contribution to the Schottky heat capacity below 350 K.

Carlson and Dieke[45,46] have determined the energy levels of (0.2 and 2 mass per cent) Nd^{3+}-doped $LaCl_3$ from fluorescence and absorption spectra at 4 and 77 K. The Stark levels of the $^4I_{9/2}$ ground J-manifold are listed in table 1. (Stark levels of the $^4I_{11/2}$ J-manifold were included in the Schottky calculation, although they are not listed.) The spectroscopic Schottky contribution, calculated from the Nd^{3+}-doped $LaCl_3$ levels, is shown as a solid line in figure 4.

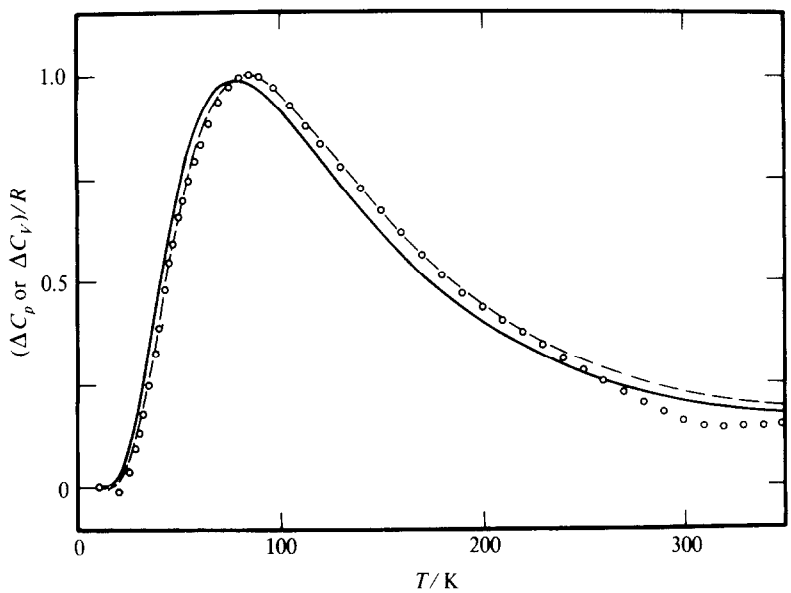

FIGURE 4. The Schottky contribution for $NdCl_3$. ———, Nd^{3+}-doped $LaCl_3$ spectroscopic Schottky contribution; ○, concentrated $NdCl_3$ calorimetric Schottky contribution; - - -, the Schottky contribution calculated from the calorimetrically deduced energy levels (see text).

The $NdCl_3$ lattice heat capacity was estimated by the weighted sum:

$$C_p(\text{lattice, } NdCl_3) = 0.43C_p(LaCl_3) + 0.57C_p(\text{lattice, } GdCl_3).$$

The weighting factors were derived using equation (2). The calorimetric Schottky curve derived through use of the above approximate lattice contribution is represented by the open circles of figure 4. Below approximately 250 K there is clearly a shift of the calorimetric Schottky contribution to higher temperatures relative to the spectroscopic curve, as would be expected due to the stronger crystal field within concentrated $NdCl_3$ relative to that in the $LaCl_3$ host. That the maximum Schottky peak height is nearly identical for the spectroscopic and calorimetric Schottky curves implies that the fractional shift in the $^4I_{9/2}$ Stark level energies may be estimated from the fractional shift in the temperature of the Schottky maximum, as

shown earlier (see figure 1a). The relative splittings of the $^4I_{9/2}$ levels of concentrated $NdCl_3$ are not expected to be identical to those found for Nd^{3+}-doped $LaCl_3$; however, with the aid of figure 1b, the relative splittings are maintained as constant as possible, while attempting to fit the calorimetric Schottky curve. The Stark levels of concentrated $NdCl_3$ derived in this manner, which yield the best agreement between the calculated and calorimetric Schottky curves, are listed in table 1. (The calculated Schottky contribution is represented by the dashed curve in figure 4.) The uncertainty in these energies is estimated to be approximately 3 per cent of the separation from the ground state. Above 230 K, some of the observed deviation may be occasioned by compression of the ground J-manifold due to expansion of the lattice; however, the deviation is much too large and sudden to be fully accounted for by this effect.

$SmCl_3$. The Schottky contribution to the heat capacities of all Sm(III) compounds below about 200 K is primarily due to thermal population of the excited Stark levels of the $^6H_{5/2}$ ground [SL]J-manifold. Near 150 K, population of the first excited [SL]J-manifold, centered near 1000 cm^{-1}, begins to make an appreciable contribution to the Schottky heat capacity and ultimately causes the Schottky curve to rise again after the first maximum (see figure 5).

The energy levels of (0.2 and 2 mass per cent) Sm^{3+}-doped $LaCl_3$ were determined by Magno and Dieke[49] from absorption and fluorescence spectra at 4 and 77 K. The Stark levels of the $^6H_{5/2}$ and $^6H_{7/2}$ [SL]J-states are listed in table 1. The $^6H_{9/2}$ [SL]J-manifold, centered near 2300 cm^{-1}, was included in the Schottky heat-capacity calculation; however, its contribution is very small below 350 K. The spectroscopic Schottky contribution calculated from the energy levels of Sm^{3+}-doped $LaCl_3$ is shown as a solid line in figure 5.

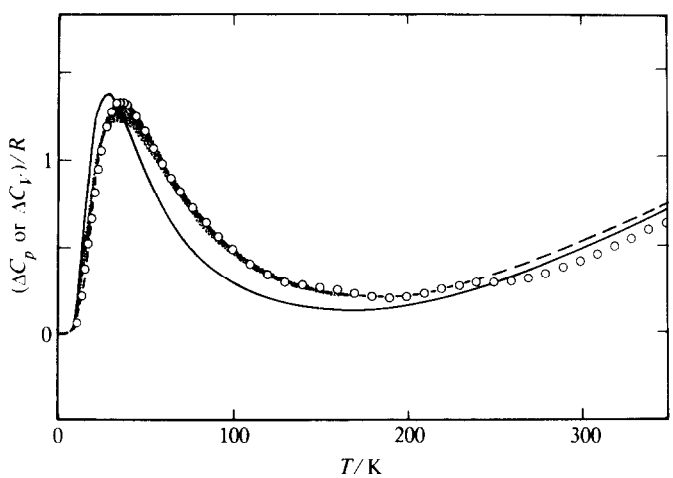

FIGURE 5. The Schottky contribution for $SmCl_3$. ——, Sm^{3+}-doped $LaCl_3$ spectroscopic Schottky contribution; ○, concentrated $SmCl_3$ calorimetric Schottky contribution; · · · · ·, the Schottky contribution calculated from the calorimetrically deduced energy levels (see text). The shaded region represents the Schottky contribution calculated from the electronic Raman scattering results of this research. The width of the band reflects the ± 3 cm^{-1} uncertainty in these wavenumbers.

The lattice heat capacity of $SmCl_3$ was approximated by

$$C_p(\text{lattice, } SmCl_3) = 0.21C_p(LaCl_3)+0.79C_p(\text{lattice, } GdCl_3).$$

The weighting factors were derived using equation (2). The calorimetric Schottky contribution derived by subtracting the above approximate lattice contribution from the total $SmCl_3$ heat capacity is represented by the circles in figure 5. In complete analogy to the $NdCl_3$ result, the Schottky maxima in C_p/R agree within 0.015, while below 230 K the calorimetric curve is clearly shifted to higher temperatures relative to the spectroscopic Schottky contribution. The relatively low energy of the first two excited Stark levels causes the $SmCl_3$ Schottky heat capacity to be particularly sensitive to small shifts in their energies. The effect of the stronger crystal field of concentrated $SmCl_3$ relative to that in the $LaCl_3$ host is readily apparent in figure 5. The Stark levels of the $^6H_{7/2}$ manifold are much too high in energy for small shifts in their positions to have any appreciable effect on the observed Schottky heat capacity. The entire observed shift may, therefore, be assumed to be due to energy-level shifts within the $^6H_{5/2}$ [SL]J-manifold. The magnitudes of the shifts were estimated by the same technique used for the $^4I_{9/2}$ levels in $NdCl_3$. Excellent agreement is obtained between the calculated and spectroscopic Schottky heat capacities below 230 K when the two excited Stark-level wavenumbers are adjusted by 10 and 22 cm^{-1}. The energy levels of the $^6H_{5/2}$ [SL]J-manifold of Sm^{3+}-doped $LaCl_3$ (the filled circles) and those estimated here for concentrated $SmCl_3$ (the open circles) are shown in figure 1c. These energy levels are also listed in table 1. The agreement between the calorimetric and adjusted spectroscopic Schottky heat capacities is particularly satisfying in view of the fact that the adjustment involved only two levels and yielded excellent agreement over a range of 230 K. Above 230 K the calorimetrically deduced curve trends below the calculated curves as was previously observed for both $EuCl_3$ and $NdCl_3$.

$PrCl_3$. The analysis of the Schottky contribution to the heat capacity of $PrCl_3$ is complicated by unusual shifts in the Stark-level energies as the intensity of the crystalline field is varied. However, the basic arguments remain essentially unchanged from those applied to the preceding compounds.

The energy levels of Pr^{3+}-doped $LaCl_3$ were determined from absorption and fluorescence spectra by Sarup and Crozier.[50] The energies of the Stark levels arising from the $^3H_4$ ground [SL]J-manifold are listed in table 1. The Stark levels of the $^3H_5$ [SL]J-manifold were also included in the spectroscopic Schottky calculation, although they do not appear in the table. The Schottky curve calculated from the Pr^{3+}-doped $LaCl_3$ energy levels is shown as a solid line in figure 6.

The lattice heat capacity of $PrCl_3$ was approximated by the weighted sum:

$$C_p(\text{lattice, } PrCl_3) = 0.54C_p(LaCl_3)+0.46C_p(\text{lattice, } GdCl_3).$$

The weighting factors were determined using equation (2). The derived calorimetric Schottky contribution is represented by the circles in figure 6. The most striking difference between the $PrCl_3$ results and those for all previous compounds is the obvious lack of agreement between the calorimetric and spectroscopic Schottky maxima. The calorimetric curve for C_p/R is approximately 0.075 below the

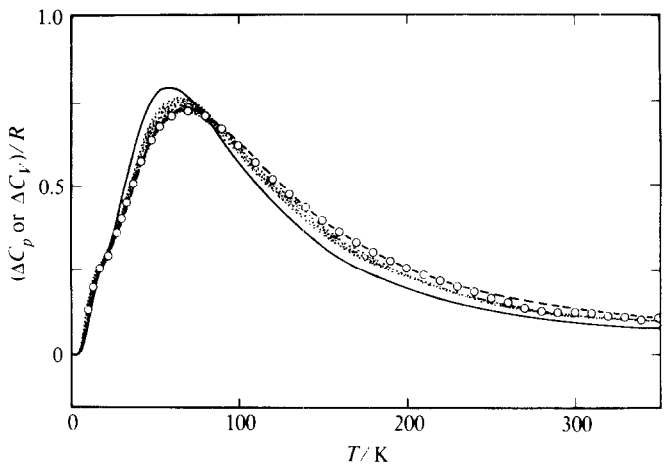

FIGURE 6. The Schottky contribution for $PrCl_3$. ———, Pr^{3+}-doped $LaCl_3$ spectroscopic Schottky contribution; ○, concentrated $PrCl_3$ calorimetric Schottky contribution; , the Schottky contribution calculated from the calorimetrically deduced energy levels (see text). The shaded region represents the Schottky contribution calculated from the electronic Raman scattering results of this research. The width of the band reflects the ± 3 cm^{-1} uncertainty in these wavenumbers.

spectroscopic curve at the maximum. Such a result, however, is anticipated since McLaughlin and Conway[52] have shown that the energy of the first excited Stark level ($\mu = 3$) of Pr^{3+} decreases monotonically for Pr^{3+} doped successively into $LaCl_3$, $CeCl_3$, $NdCl_3$, $SmCl_3$, and $GdCl_3$. McLaughlin and Conway unfortunately were unable to observe any of the upper-four Stark levels of the $^3H_4$ ground [SL]J-manifold.

Dorman[51] has determined the Stark splitting of the first two excited Stark levels ($^3H_4$, $\mu = 3^-$ and $2'$) for dopant Pr^{3+} in $LaCl_3$ crystals ranging from 0.26 to 100 mass per cent from their absorption spectra. The variation in wavenumber is not monotonic; however, comparison of the 0.26 and 100 mass per cent results shows the $\mu = 3^-$ level to have shifted from 33.3 to 31.8 cm^{-1}, while the $\mu = 2'$ level has shifted from 95.9 to 99.5 cm^{-1}. In view of the findings of McLaughlin and Conway,[52] Dorman's results are reasonable. The first excited Stark-level energy is decreased, while the second excited level increases in energy as would normally be expected due to the stronger crystal field of $PrCl_3$. Due to overlap with the vibronic spectrum, Dorman was unable to observe the upper-three Stark levels of the $^3H_4$ [SL]J-manifold. If these upper levels shift to higher energies in the concentrated salt, the most obvious effect on the Schottky heat capacity would be a lowering of the maxima. It is, therefore, postulated that such a shift is the cause of the depressed calorimetric Schottky maximum in figure 6. Energies of the upper-three Stark levels of the $^3H_4$ J-manifold for concentrated $PrCl_3$ were evaluated by holding constant the energies of the first two excited Stark levels determined by Dorman, while the remaining Stark-level energies were increased until good agreement between the calculated and calorimetric Schottky heat capacities was obtained. Wavenumber shifts of approximately 25 to 35 cm^{-1} were necessary to achieve good agreement. Figure 1d

shows the Stark splitting of the $^3H_4$-manifold for Pr^{3+}-doped $LaCl_3$ (●) and the estimated splitting for concentrated $PrCl_3$ (□). The ▮'s represent the energy levels determined by Dorman. The Schottky contribution calculated using the energy levels estimated for concentrated $PrCl_3$ are shown as a dashed curve in figure 6. The calorimetric Schottky heat capacity does trend below the calculated curve near 230 K; however, the magnitude of the deviation is much less than for any of the previous compounds.

It is interesting to compare the Schottky curves found here for Pr^{3+}-doped $LaCl_3$ and concentrated $PrCl_3$ with that deduced for concentrated $Pr(OH)_3$.[1] If the three Schottky curves were shown in the same figure, a gradual shift of the Schottky maximum to higher temperatures and lower heat capacities would be observed. Indeed, the first excited wavenumber level of $Pr(OH)_3$ shifts so low (to about 11 cm^{-1}) that a second Schottky maximum occurs near 7 K.

5. Crystal-field parameters for concentrated trichlorides

In order to corroborate the magnitudes of the shifts estimated in the previous section, crystal-field calculations, which included the effects of intermediate coupling and J-mixing between the ground and first excited states, were performed.

The Hamiltonian for a lanthide ion at a site of C_{3h} symmetry is given as

$$H = H_0 + (B_2^0 V_2^0 + B_4^0 V_4^0 + B_6^0 V_6^0 + B_6^6 V_6^6),$$

in which H_0 is the free-ion Hamiltonian and the remaining terms describe the effect of the crystalline environment. The crystal-field parameters—B_2^0, B_4^0, B_6^0, and B_6^6—have been defined and normalized according to the procedures of Stevens,[53] of Elliot and Stevens,[54] and of Judd.[55] Configuration interaction processes give rise to effects that cannot be included in the crystal-field parameters as defined above; however, because the principal effect of these processes is to shift the centers of gravity of excited [SL]J-manifolds, they have little effect on the crystal-field splitting of the ground [SL]J-state. For this reason, no attempt has been made to include the effect of configuration interaction in the calculations presented here. Because the lowest several J-states are essentially unaffected by intermediate coupling,[6] properties calculated for these states yield the most meaningful results when theory and experiment are compared. The discrepancy between calculated and spectroscopically determined energy levels is typically less than about 4 per cent (see reference 1).

The crystal-field calculations were performed to demonstrate that sets of crystal-field parameters for concentrated $PrCl_3$, $NdCl_3$, and $SmCl_3$ could be deduced with the following properties: (1), energies of Stark levels derived from the crystal-field parameters are in good agreement with spectroscopically-determined Stark-level energies of the concentrated compound; (2), the variations of the crystal-field parameters across the lanthanide series parallel that found for other series with lanthanide ions at sites of C_{3h} point symmetry; (3), Schottky contributions calculated from energy levels derived from the crystal-field parameters are in good agreement with the calorimetrically derived Schottky heat capacity. The rationale employed in their determination follows.

Three Kramers doublets result from the crystal-field splitting of the $^6H_{5/2}$ ground [SL]J-state of $SmCl_3$. From the calorimetrically derived Schottky curve (figure 5) the wavenumbers of the two excited Stark levels were ascertained to be near 50 and 88 cm^{-1}. The more complex ground [SL]J-manifolds of $PrCl_3$ and $NdCl_3$ make estimation of their energy levels much less certain. If only the "first-order" calculation is considered (*i.e.* neglect of J-mixing with the $^6H_{7/2}$ J-state), the two excited Stark level energies can be used to define uniquely B_2^0 and B_4^0 for $SmCl_3$. B_6^0 and B_6^6 are not involved in the $^6H_{5/2}$ first-order calculation. B_2^0 and B_4^0 for $NdCl_3$ and $PrCl_3$ were then estimated by paralleling the variations in the crystal-field parameters found for other series.

Three series involving lanthanide ions in sites of C_{3h} symmetry have been studied in detail by optical spectroscopy. The deduced crystal-field parameters for most of the trivalent lanthanide ions doped into $LaCl_3$ and for most of the concentrated lanthanide ethyl sulfate nonahydrates have been tabulated by Dieke.[1] The available crystal-field parameters for the concentrated lanthanide trihydroxides are listed in table 2. Because the crystal-field parameters of the Ln^{3+}-doped $LaCl_3$ are a function

TABLE 2. Spectroscopically deduced crystal-field parameters B_n^m for the lanthanide trihydroxides

Ln	B_2^0/cm^{-1}	B_4^0/cm^{-1}	B_6^0/cm^{-1}	B_6^6/cm^{-1}	Reference
Ce					
Pr	237±5	−85±3	−52±2	590±20	1
Nd					
Pm					
Sm					
Eu	211±11	−71±8	−54±3	617±30	56
Gd	183±11	−57±8	−85±25	840±140	56
Tb	208±3	−69±2	−45±1	585±12	27
Dy	209±7	−76±4	−40±2	542±27	56
Ho					
Er	192±6	−64±3	−40±1	521±8	57
Tm					

of the dopant mass fraction and because the large anions of $Ln(EtSO_4)_3 \cdot 9H_2O$ may give rise to important steric effects, the results for the lanthanide trihydroxides were weighted most heavily, when the paralleling of the trends in the crystal-field parameters was attempted. As seen in table 2, the variations in these crystal-field parameters across the series are generally quite subtle—discounting $Gd(OH)_3$ although the variations are not monotonic, some dominant trends are apparent.

The B_6^0 and B_6^6 values for $NdCl_3$ and $PrCl_3$ were estimated with the approximate energy levels of the previous section as a guide once B_2^0 and B_4^0 had been estimated. The B_6^0 and B_6^6 values for $NdCl_3$ and $PrCl_3$ then allowed estimation of these parameters for $SmCl_3$. With the complete sets of "first-order" crystal-field parameters, the effect of J-mixing with the first excited [SL] J-state of each compound was calculated. The ground [SL]J-manifold crystal-field splittings of $PrCl_3$ and $SmCl_3$ were shifted only slightly by the J-mixing calculation. The maximum shift, relative to the ground state, observed for either compound was

3 cm^{-1}. The mean shift was less than 2 cm^{-1}. In contrast, due to a very large J-mixing effect upon the ground Stark level ($\mu = 5/2$), the four excited states of the $^4I_{9/2}$ [SL]J-manifold of $NdCl_3$ shifted to higher wavenumbers by about 10 cm^{-1}. Small changes in the crystal-field parameters leave the effect of J-mixing upon any particular Stark level virtually unchanged. By means of an essentially iterative technique, small adjustments were made in the crystal-field parameters until the three criteria, stated at the beginning of this section, were met. The insensitivity of J-mixing to small changes in the crystal-field parameters held to a minimum the number (two) of iterations required. The deduced sets of crystal-field parameters of concentrated $SmCl_3$, $NdCl_3$, and $PrCl_3$ are listed in table 3. The uncertainty in the deduced crystal-field parameters is estimated to be approximately 2 per cent. The maximum in the B_6^6 value of $NdCl_3$ was incorporated to parallel the observed trend in B_6^6 for the concentrated ethyl sulfate series and for the doped $LaCl_3$ crystals.

TABLE 3. Deduced crystal-field parameters B_n^m for several concentrated lanthanide trichlorides

Compound	B_2^0/cm^{-1}	B_4^0/cm^{-1}	B_6^0/cm^{-1}	B_6^6/cm^{-1}
$PrCl_3$	120	−28	−38	525
$NdCl_3$	118	−27	−37	535
$SmCl_3$	114	−26	−36	525

The energy levels of the ground [SL]J-manifolds of $PrCl_3$, $NdCl_3$, and $SmCl_3$ calculated from the estimated crystal-field parameters are listed in table 1. The Schottky heat capacities calculated from the energy levels derived from the crystal-field parameters and from the extrapolated Ln^{3+}-doped $LaCl_3$ crystal-field splitting are nearly identical. For this reason no additional curves are shown in figures 4 to 6. The energy levels calculated from the estimated crystal-field parameters were added to figures 1b and 1d. (For $SmCl_3$ the method used to determine the crystal-field parameters required that the calculated energy levels equalled those deduced earlier from the nearly linear extrapolation of the Sm^{3+}-doped $LaCl_3$ crystal-field splitting. Therefore, no additional energy levels appear in figure 1c.)

6. Spectral results for concentrated trichlorides

ABSORPTION EXPERIMENTS

Spectral studies of concentrated salts have generally been neglected to avoid complexities of broadened bands and satellite structures. Although numerous absorption and fluorescence studies have been performed upon Ln^{3+}-doped $LaCl_3$ crystals,[6] only two such experiments have been performed upon the concentrated salts. Of these, only one yields the complete Stark splitting of the ground [SL]J-manifold.

The absorption study of Dorman,[51] which yielded two of the five excited $^3H_4$ Stark levels of concentrated $PrCl_3$, was described earlier. Only for $NdCl_3$ has the complete crystal-field splitting of the ground J-manifold been deduced from

absorption spectra.[47,48] The Stark levels of the ground [SL]J-manifold of concentrated $PrCl_3$ deduced by Dorman[50] and that of concentrated $NdCl_3$ deduced by Prinz[47,48] are listed in table 1 and shown in figures 1a and 1b, respectively.

ELECTRONIC RAMAN SCATTERING EXPERIMENTS

Electronic Raman scattering experiments have been carried out on single crystals of $PrCl_3$ and $SmCl_3$. Single crystals of these compounds were grown by standard techniques.[58–60] Samples were repeatedly passed through a Bridgman zone-furnace to anneal the crystal and reduce defects and dislocations to a minimum. The crystals were carefully polished in a dry box and mounted in optically transparent cells with holders that exposed the sample to excitation sources either parallel or perpendicular to the C_3 axis for polarization studies.

Excitation sources included the traditional A–H6 high-pressure mercury arc used to repeat the earlier experiments of Hougen and Singh[15] on $PrCl_3$. $PrCl_3$ crystals do not absorb the 253.7 nm radiation, which has many advantages for the excitation of Raman spectra. Sources used for $SmCl_3$ experiments include a high-powered (4 W) continuous or pulsed ruby laser (694.3 nm) and a c.w. helium–neon gas laser (632.8 nm). $SmCl_3$ crystals do not absorb the laser light directly at these frequencies although some two-photon absorption is possible. Samples were cooled to 85 K using a liquid-nitrogen-filled conduction Dewar. A heat shield and optical filters were used to reduce radiation scattered into the spectrometer from other laboratory sources.

The Raman spectra were recorded with a 1.0 m McPherson Czerny–Turner spectrograph–spectrophotometer equipped with a 1100 mm^{-1} grating and plate factor of 8×10^7 in first order. The optical path length of the crystals was up to 1.0 cm in some cases and exposure times ranged from 4 to 12 h. Photographic plates were sensitized to maximize the possibility of observing the expected faint lines or bands. Bandwidths observed for $PrCl_3$ are comparable with those reported by Hougen and Singh.[15]

The Raman-active lattice-vibrational transitions were also observed for single crystals of $LaCl_3$, $PrCl_3$, $NdCl_3$, and $SmCl_3$ at 300 K and at 85 K. Excitation sources used were the same as those for electronic Raman measurements. Only the vibrational transitions in $NdCl_3$ could be identified readily, although at 85 K it is possible that one or two excited Stark levels were observed weakly since their frequencies agree within experimental error with values reported from absorption measurements. Transitions were identified with the aid of data and analyses reported by Richman, Satten, and Wong,[10] by Murphy, Caspers, and Buchanan,[11] and by Cohen, Riseberg, and Moos.[12] For $LnCl_3$ the 300 K spectra yield five Stokes and five anti-Stokes Raman lines with wavenumber shifts less than 250 cm^{-1}. These lines are consistent with the polarizations and assignments reported earlier.[15] Electronic Raman lines were observed only at the lower temperature (85 K). Table 4 presents a compilation of all observed vibrational Raman wavenumbers at 300 and 85 K. The vibrational levels shift in going from $PrCl_3$ to $SmCl_3$ as would be expected for changes in ionic size and molar volume. The deduced electronic energy levels for the

TABLE 4. Observed vibrational Raman wavenumbers σ for $LnCl_3$ at 300 and 85 K

	La		Pr		Nd		Sm	
T/K	300	85	300	85	300	85	300	85
Symmetry species	σ/cm^{-1}							
E_{2g}	105	108	103	106	103	106	102	104
A_g	174	178	177	183	178	183	180	183
E_{1g}	181	186	186	197	186	191	187	191
E_{2g}	205	211	213	216	214	217	218	220
E_{2g}	212	218	217	220	218	224	225	230

ground and first excited [SL]J-manifolds of $PrCl_3$ and $SmCl_3$ are also listed in table 1.

Electronic Raman scattering also reveals evidence of Sm^{2+} in the single-crystal $SmCl_3$ although the intensities are weaker by a factor of 100. In certain cases there appear to be weak lines possibly associated with a second Sm^{3+} site arising from the local distortions in the lattice caused by the presence of Sm^{2+}. Although less than 0.1 per cent of the samarium ions are divalent in the spectroscopic samples, this results in some samarium trivalent ions being subject to a somewhat different (lower) symmetry, which gives rise to a larger CEF splitting of the ground-state manifold ($^6H_{5/2}$) for these ions such as one observed for Sm^{3+} in LaF_3 [$\mu(\pm 1/2) = 0$, $\mu(\pm 3/2) = 45$ cm^{-1}, $\mu(\pm 5/2) = 159$ cm^{-1}].

7. Comparison of spectroscopic and calorimetric results

If allowance is made for the uncertainties in the energy levels deduced from extrapolations of the Nd^{3+}-doped $LaCl_3$ crystal-field splitting (about 3 per cent) and those derived from estimated crystal-field parameters (about 4 per cent) excellent agreement is observed between these values and those deduced by Prinz from the absorption spectrum of concentrated $NdCl_3$. As figure 4 shows, excellent agreement is achieved from 5 K to approximately 230 K.

The crystal-field splitting deduced from the electron Raman scattering results for concentrated $SmCl_3$ and $PrCl_3$ is clearly greater than that found for the corresponding doped $LaCl_3$ crystals; however, due to the uncertainty of about ± 3 cm^{-1} in the spectroscopic results, unequivocal corroboration of the calorimetrically derived Schottky curves is not possible. The Schottky contributions calculated from the electronic Raman spectra are represented by the bands in figures 5 and 6. Although it is not possible to determine spectroscopically whether the weak line at 79 or 93 cm^{-1} is the true $\mu = 5/2$ electronic level, on the basis of the calorimetric results, the 93 cm^{-1} value is favored. This higher wavenumber was used in the calculation of the spectroscopic Schottky curve shown in figure 5. The 79 cm^{-1} line may be due to the presence of Sm^{2+} as previously mentioned. In spite of the uncertainties in the spectroscopic measurements, the calorimetric and spectroscopic Schottky heat capacities are in far better agreement when the wavenumbers deduced from the electronic Raman results—rather than those obtained for Ln^{3+}-doped $LaCl_3$—are used in the spectroscopic Schottky calculation.

8. Conclusions

The volumetric lattice heat-capacity approximation technique was applied to the light anhydrous lanthanide trichlorides. As anticipated, only for $EuCl_3$ was the calorimetrically derived Schottky contribution in good agreement with that calculated from Ln^{3+}-doped $LaCl_3$ energy levels and degeneracies. Here the energy levels contributing to the Schottky heat capacity below 350 K are too high in energy for small shifts in their positions to be detectable in the calorimetrically derived Schottky heat capacity. Observed discrepancies were attributable to the weak crystalline field in the $LaCl_3$ host relative to that in the concentrated salt. The energy levels of the concentrated $PrCl_3$, $NdCl_3$, and $SmCl_3$ are estimated from those of the corresponding Ln^{3+}-doped $LaCl_3$ crystals by making use of several previously unexploited properties of the Schottky heat-capacity function. To obtain corroboration of the postulated relative Stark-level shifts, sets of self-consistent crystal-field parameters—whose derived energies yield Schottky curves in excellent agreement with those derived calorimetrically—were deduced. Further applications of estimated crystal-field parameters to the resolution of Schottky heat capacities from calorimetric data may be found elsewhere.[3] Finally, the calorimetrically derived Stark levels for the concentrated salts are compared with those deduced from absorption spectra for $NdCl_3$ and electronic Raman scattering results for $SmCl_3$ and $PrCl_3$. Excellent agreement was obtained for $NdCl_3$, while the calorimetrically deduced Stark splittings for $PrCl_3$ and $SmCl_3$ were somewhat greater than those observed in the electronic Raman scattering experiments. However, all Schottky contributions calculated from spectroscopic results obtained for the concentrated lanthanide trichlorides were in far better agreement with the calorimetrically deduced curves than were the corresponding contributions calculated from the energy levels of Ln^{3+}-doped $LaCl_3$ crystals. Little evidence for shifts of the Stark-level energies with temperature is noted in the Schottky curves; however, at high temperatures where this effect is expected to be most important, the uncertainties in the measured heat capacities tend to preclude detection of this effect.

The authors appreciate the cooperation of Professor H. M. Crosswhite in providing the absorption spectra essential to the corroboration of the calorimetric Schottky contribution for $NdCl_3$. One of us (R.D.C.) thanks the Ethyl Corporation for a fellowship award.

REFERENCES

1. Chirico, R. D.; Westrum, E. F., Jr.; Gruber, J. B.; Warmkessel, J. *J. Chem. Thermodynamics* **1979,** 11, 835.
2. Chirico, R. D.; Westrum, E. F., Jr. *J. Chem. Thermodynamics* **1980,** 12, 71.
3. Chirico, R. D.; Westrum, E. F., Jr. *J. Chem. Thermodynamics* **1980,** 12, 311.
4. Sommers, J. A.; Westrum, E. F., Jr. *J. Chem. Thermodynamics* **1976,** 8, 1115.
5. Sommers, J. A.; Westrum, E. F., Jr. *J. Chem. Thermodynamics* **1977,** 9, 1.
6. Dieke, G. H. *Spectra and Energy Levels of Rare Earth Ions in Crystals*. Crosswhite, H. M.; Crosswhite, Hannah: editors. Interscience: New York. **1968.**
7. Cohen, E.; Moos, H. W. *Phys. Rev.* **1967,** 161, 258.
8. Cohen, E.; Moos, H. W. *Phys. Rev.* **1967,** 161, 268.

9. Scott, P. D.; Meissner, H. E.; Crosswhite, H. M. *Phys. Lett.* **1969,** 28A, 489.
10. Richman, I.; Satten, R. A.; Wong, E. Y. *J. Chem. Phys.* **1963,** 39, 1833.
11. Murphy, J.; Caspers, H. H.; Buchanan, R. A. *J. Chem. Phys.* **1964,** 40, 743.
12. Cohen, E.; Riseberg, L. A.; Moos, H. W. *Phys. Rev.* **1967,** 157, 252; **1968,** 175, 521.
13. Sibaiya, L.; Venkataramiah, H. S. *Phys. Rev.* **1939,** 56, 381.
14. Sibaiya, L. *Phys. Rev.* **1941,** 60, 471; Gross, E. F.; Raskin, A. I.; Seidel, A. *Acta Physicochem. U.S.S.R.* **1941,** 13, 591.
15. Hougen, J. T.; Singh, S. *Proc. R. Soc. (Lond.) A* **1964,** 277, 193; *Phys. Rev. Lett.* **1963,** 10, 406.
16. Elliott, R. J.; Loudon, R. *Phys. Lett.* **1963,** 3, 189.
17. Axe, J. D. *Phys. Rev.* **1964,** 136, A42.
18. Judd, B. R. *Operator Techniques in Atomic Spectroscopy.* McGraw-Hill: New York. **1963.**
19. Carnall, W. T.; Fields, P. R. *Lanthanide/Actinide Chemistry,* Chapter 7. Gould, R. F.: editor. American Chemical Society: Washington, D.C. **1967.**
20. Dieke, G. H.; Crosswhite, H. M. *Appl. Optics* **1963,** 2, 675.
21. Boatner, L. A.; Abraham, M. M. *Rep. Prog. Phys.* **1978,** 41, 87.
22. Maiman, T. H. *Phys. Rev. Lett.* **1960,** 4, 564.
23. Lengyel, B. A. *Introduction to Laser Physics.* John Wiley and Sons, Inc.: New York. **1966.**
24. Abella, I. D. *Phys. Rev. Lett.* **1962,** 9, 453.
25. Singh, S.; Stoicheff, B. P. *J. Phys. Chem.* **1963,** 38, 2032.
26. Peticolas, W. L.; Norris, R.; Rieckhoff, K. E. *J. Chem. Phys.* **1965,** 42, 4164.
27. Fowler, W. B.; Dexter, D. L. *J. Chem. Phys.* **1965,** 43, 1768.
28. Dirac, P. A. M. *Proc. R. Soc. (Lond.) A* **1927,** 114, 143, 710.
29. Goeppert-Mayer, M. *Angw. Physik.* **1931,** 9, 273.
30. Kaiser, S.; Garrett, C. G. B. *Phys. Rev. Lett.* **1961,** 7, 229.
31. Richman, I.; Chang, N. C. *Appl. Phys. Lett.* **1967,** 10, 218.
32. Schaack, G.; Koningstein, J. A. *J. Opt. Soc. Am.* **1970,** 60, 1110.
33. Bayer, E.; Schaack, G. *Phys. Stat. Sol.* **1969,** 34, K115.
34. Kleinman, D. A. *Phys. Rev.* **1962,** 125, 87.
35. Stoner, T. R.; Gruber, J. B. *J. Chem. Phys.* **1970,** 52, 1508. See also Gruber, J. B. *Proc. 9th Rare Earth Research Conf.* **1971,** 2, 465.
36. Peticolas, W. L. *Ann. Rev. Phys. Chem.* **1967,** 18, 233.
37. Jones, A. C. *Anal. Chem.* **1964,** 36, 296.
38. Bonch-Bruevich, A. M.; Khodovoi, V. A. *Sov. Phys.* **1965,** 85.
39. DiBartolo, B. *Optical Interactions in Solids.* John Wiley and Sons, Inc.: New York. **1968.**
40. Gruber, J. B.; Larson, E. D.; Olsen, D. N.; Stoner, T. R. *Ann. Proc. N. D. Acad. Si.* **1978,** 31, 218.
41. Gopal, E. S. R. *Specific Heats at Low Temperatures.* Plenum Press: New York. **1966.**
42. Marquard, C. D. *Proc. Phys. Soc. (Lond.)* **1967,** 92, 650.
43. Clover, R. B.; Wolf, W. P. *Solid State Comm.* **1968,** 6, 331.
44. DeShazer, L. C.; Dieke, G. H. *J. Chem. Phys.* **1963,** 38, 2190.
45. Carlson, E. H.; Dieke, G. H. *J. Chem. Phys.* **1958,** 29, 229.
46. Carlson, E. H.; Dieke, G. H. *J. Chem. Phys.* **1961,** 34, 1602.
47. Prinz, G. A. Doctoral Dissertation. Johns Hopkins University: Baltimore, Md. **1966.**
48. Prinz, G. A. *Phys. Rev.* **1966,** 152, 474.
49. Magno, M. S.; Dieke, G. H. *J. Chem. Phys.* **1962,** 37, 2354.
50. Sarup, R.; Crozier, M. H. *J. Chem. Phys.* **1965,** 42, 371.
51. Dorman, E. *J. Chem. Phys.* **1966,** 44, 2910.
52. McLaughlin, R. D.; Conway, J. G. *J. Chem. Phys.* **1963,** 38, 1037.
53. Stevens, K. W. H. *Proc. Phys. Soc. (Lond.) A* **1952,** 65, 209.
54. Elliot, R. J.; Stevens, K. W. H. *Proc. R. Soc. (Lond.) A* **1953,** 218, 553.
55. Judd, B. R. *Proc. R. Soc. (Lond.) A* **1955,** 227, 552.
56. Cone, R. L.; Faulhaber, R. *J. Chem. Phys.* **1971,** 55, 5198.
57. Cone, R. L. *J. Chem. Phys.* **1972,** 57, 4893.
58. Hutchison, C. A., Jr.; Wong, E. Y. *J. Chem. Phys.* **1958,** 29, 754.
59. Sayre, E. V.; Sancier, K. M.; Freed, S. *J. Chem. Phys.* **1955,** 23, 2060.
60. Dieke, G. H.; Sarup, R. *J. Chem. Phys.* **1958,** 29, 741.